Int. J. Electrochem. Sci., 17 **(2022)** Article Number: 220755, doi: 10.20964/2022.07.58

International Journal of
ELECTROCHEMICAL
SCIENCE
www.electrochemsci.org

Short Communication

First principles study on photoelectric properties of Tl-doped $CuInS_2$ solar cell materials

Dongwei Zhang, Wenyu Dong, Yinsheng Yu, Junjie Zhou[*]

School of Mechanical and Power Engineering, Zhengzhou University, Zhengzhou 450001, China
[*]E-mail: zhoujj@zzu.edu.cn

Received: 9 April 2022 / *Accepted:* 18 May 2022 / *Published:* 6 June 2022

As a direct energy gap I-III-VI semiconductor compound material, copper indium sulfur semiconductor thin film (CIS) has the significant advantages of high light absorption coefficient, thin thickness and low band gap, which is suitable for the preparation of photoelectric converter devices, and thus it has great potential in the field of thin-film solar cells. In this paper, the calculation models of protocell CIS and CIS doped with Tl (CIS:Tl) materials were constructed. The electronic structure and optical properties of protocell CIS and CIS:Tl materials were obtained by using the first principle calculation method. The calculation results show that both protocell CIS and CIS:Tl are direct band gap semiconductors, and it was found that doping Tl in CIS can adjust the band gap value of the electronic structure of semiconductor materials, so that the optimal band gap width of the solar absorption spectrum was achieved. The band gap of CIS:Tl material is 33.4% lower than that of protocell CIS. In addition, doping Tl can shifts the absorption peak of CIS to the high-energy region, and the absorption intensity of the main solar absorption peak is increased by 8.4%, which significantly enhances the light absorption capacity of copper indium sulfur semiconductor solar cells. Compared with the original cell CIS, the real peak of conductivity of Tl doped CIS is increased by 10.06%, which effectively improves the crystallization degree of the film and the efficiency of solar cells.

Keywords: CIS semiconductor thin films, first principles, doping, electronic structure, optical properties.

1. INTRODUCTION

With China's "carbon peak" and "carbon neutral" goals, the development and use of renewable energy has become an important pathway to achieve low carbon development in China, and the development and use of solar energy as a rich renewable energy source is gradually gaining attention. As a carrier of energy storage, the development and application of solar cells is taking a new step forward. At present, monocrystalline silicon solar cells have the highest conversion efficiency in the laboratory, but they are expensive and difficult to produce on a large scale. Secondly, the photovoltaic conversion

effect of CdTe polycrystalline thin film cell is also relatively good, but it can not become an ideal solar cell because of the high toxicity of cadmium. And $CuInS_2$ (CIS), with its low preparation cost, large light absorption coefficient and suitable forbidden band width, has a wide range of application prospects in large-scale industrial preparation and solar electric vehicles. Although some research progress has been made in the design and preparation of CIS materials, the microscopic mechanism of their performance regulation is still unclear. Currently, research on copper-indium-sulfur semiconductor thin films has focused on the design and preparation of different components of CIS under experimental conditions and the exploration of CIS performance regulation. In contrast to experimental studies, theoretical calculations have focused on the effects of intrinsic defects and the adjustment of cation ratios in components on the electronic structure and optical properties of CIS. It has a wide range of applications in the numerical prediction and microscopic study of material properties. There is limited research on the effect of Tl doping of In's cognate element, group IIIA, on CIS properties using the first principles approach.

Castro [1] proposed the conclusion that the luminescence originates from intrinsic defects in the nanocrystal structure of thin film semiconductors. The experimental data observed by Omata [2] and Kraatz [3] are consistent with localized states and transitions between valence bands. Chen et al used a first-nature principle study [4] to calculate the jump energies of various point defects in CIS using density generalized theory. Rice [5] used magnetic circular dichroism to identify the presence of Cu^{2+} in CIS thin-film semiconductors, attributing the luminescence to impurity atoms. The ternary nature of CIS allows further control of its band gap by adjusting the cation ratio. This was demonstrated by Uehara [6], who changed the CIS semiconductor film composition by adjusting the concentration of Cu^{2+} precursors present in the synthesis from Although the semiconductor thin film crystal size does not change, the peak absorption and the wavelength of the fluorescence peak of the semiconductor thin film crystal decrease with the increase of the band gap as the Cu/In ratio decreases. For CIS, the valence band is generated by the hybridization of the Cu d-orbitals and the anion p-orbitals with a binding energy of about 2.5 eV [7, 8]. For $CuInSe_2$, it has been shown that a decrease in Cu concentration, accompanied by a corresponding decrease in Cu d-orbitals properties, leads to a decrease in Cu d-/Se p-band inter-rejection, which reduces the valence band maximum of the material [9].Choi [10] showed that the doping of small amounts of Zn^{2+} leads to lattice shrinkage, while the addition of Cd^{2+}, whose ionic radius is larger than that of In^{3+} or Cu^{+} 1/3 larger [11], leading to induce tensile stresses. These stresses lead to changes in the band gap, resulting in blue-shifted or red-shifted luminescence, respectively. Intrinsic point defects in CIS lead to the creation of new energy levels in the forbidden band, causing the material to have intrinsic self-doping properties [12]. Therefore, CIS thin film materials with different conductivity types can be obtained by preparing different elemental ratios. Park [13] prepared CIS thin films by vacuum evaporation with electron beam as the heating source, and the efficiency of heterojunction solar cells prepared using it was 5.6%.Siemer [14] used magnetron sputtering method to prepare CIS thin films, and the efficiency of the prepared Mo substrate/CIS/Cds /ZnO cells with an efficiency of 11.4%. Yuan Jiongliang [15] prepared copper-indium precursor films using a three-electrode deposition technique, after which the CIS films were obtained by sulfiding them.As a result, CIS semiconductor thin-film crystals have now achieved a high level of synthetic control, allowing the selection of the appropriate shape, structure and size. Furthermore, existing studies have demonstrated

the ability to tune the optical band gap and electronic properties of CIS semiconductor thin-film crystals. Tomonobu [16] studied the effect of Ga doping on the energy conversion and utilization of n-CdS / p-$CuInS_2$ thin films. The results show that Ga doping can improve the band gap and open circuit voltage of the films. After Ga doping, the energy conversion efficiency increases from 10.6% to 11.2%. However, there is a lack of a clear theoretical link between the synthesised structure and the optical properties of CIS semiconductor thin-film crystals, and the corresponding theoretical prediction methods for the optical absorption properties of CIS semiconductor thin-film crystals are seldom concerned, and the corresponding tuning tools are urgently required. In view of this, this paper investigates the photoelectric properties of CIS semiconductor thin film crystals as a solar cell material, and the first principles calculation method was used to derive the electronic structure and optical properties of CIS and CIS:Tl, and analyzes the effect of Tl element doping on CIS semiconductor thin film materials, which is expected to promote the performance optimization and application promotion of solar thin film cell materials.

2. COMPUTATIONAL MODELLING AND ASSESSMENT

2.1. Model building

In this study, the electronic structure and optical properties of CIS structure doped with Tl of the are investigated using the first principles calculation method based on the Castep module of Materials Studio software, and the effect of Tl doping on the optoelectronic properties of CIS was analysed. A structural model of CIS:Tl is shown in Fig. 1. The doping model in this section is obtained by replacing the In atom with a Tl atom, followed by geometrical and energy optimization of the replaced structural model to obtain a stable configuration.

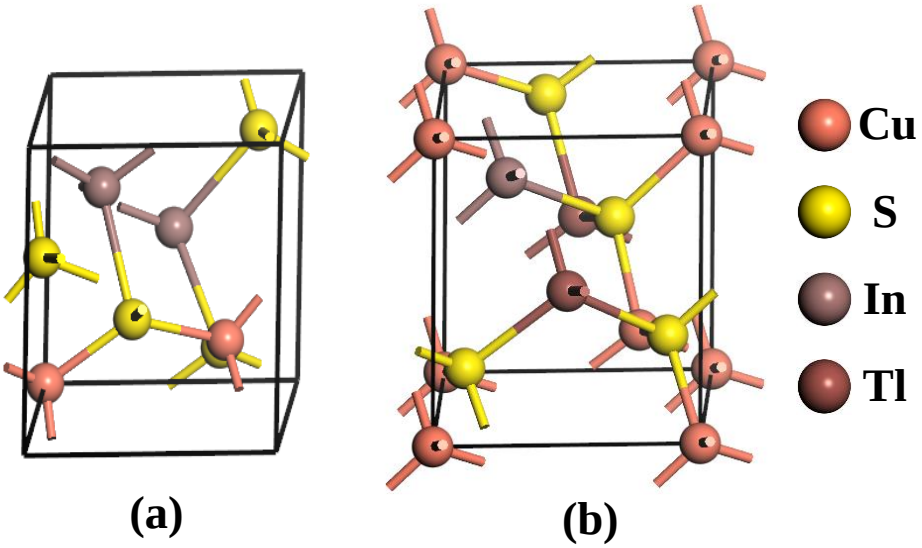

Figure 1. Microstructure model: (a) CIS, (b) CIS:Tl

2.2. Model assessment

In the first principle calculation [17], the larger the value of the truncation energy parameter, the more accurate the calculated ground state electron density is, and the more accurate the corresponding optical properties and crystal structure parameters in the system. However, a larger value of the cut-off energy generally leads to a greater additional computational resources consumed, which thus can lead to an exponential increase in the computational time. Therefore, the cut-off energy should be chosen in a appropriate way as to ensure that the results are as accurate as possible while using as little computational resources as possible. Therefore, this section assesses the truncation energy in the range of 100 eV to 600 eV, and an interval of 100 eV was assessed, as shown in Fig. 2. As can be seen from Fig. 2, when the cut-off energy of the system reaches 300 eV, the trend of its energy reduction gradually slows down, and the error is only 0.0005% at this time, which indicates that the cut-off energy above 300 eV is sufficient to ensure good first-principle calculation accuracy of the microscopic model. Taking into account the both of the computational resources and the calculation results accuracy, the cut-off energy of 500 eV was used in this paper to ensure more accurate computational results without consuming additional unnecessary computational resources.

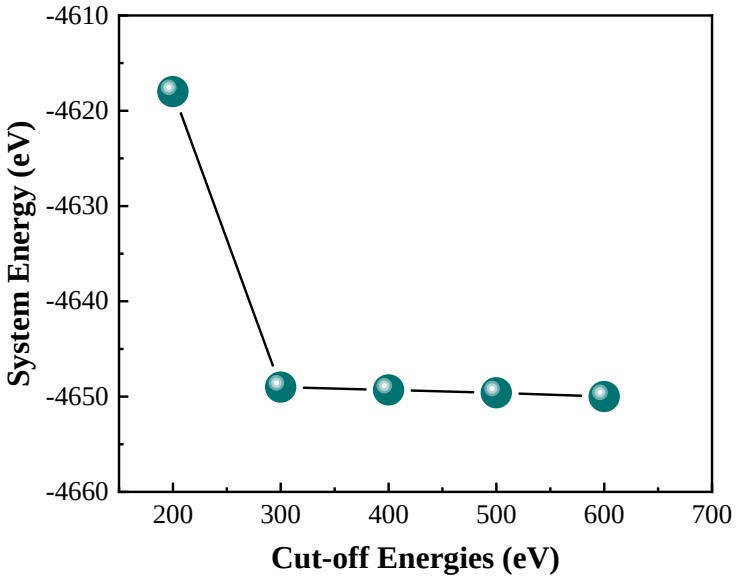

Figure 2. System energies corresponding to different cut-off energies

3. STUDY OF THE OPTOELECTRONIC PROPERTIES OF Tl-DOPED CIS

3.1. Electronic structure analysis of Tl-doped $CuInS_2$

The band structures of Tl-doped CIS and primary cell CIS were calculated, and the comparison results are shown in Fig. 3. The band gap structure next to the Fermi energy level is a good reflection of the electronic structure of a semiconductor film. Therefore, the analysis of the band gap structure next

to the Fermi energy level is used to investigate the electronic structure of the semiconductor film. A comparison of the original CIS band structure in Fig. 3a and the CIS:Tl band structure in Fig. 3b shows that the Fermi energy level of the Tl-doped CIS structure is in the same valence band region as before doping, while the top of the valence band is not affected by doping but the bottom of the conduction band appears to be shifted downwards. The doping of Tl leads to a narrowing of the band gap of the structure from 1.282 eV to 0.855 eV. It can be concluded that the doping of Tl can have an impact on the band gap value and the energy band structure of the CIS semiconductor film. It was also found that the energy bands next to the Fermi energy level of the CIS structure became sparser and the energy levels were more dispersed after Tl doping than before. The reason for this is that the corresponding impurity levels are introduced into the film structure after the elemental doping, and orbital hybridisation occurs between the energy level orbitals. Although the energy band and electronic properties of the structures show a relatively obvious change before and after the Tl doping, they are still consistent with the characteristics of a direct band gap semiconductor [18].

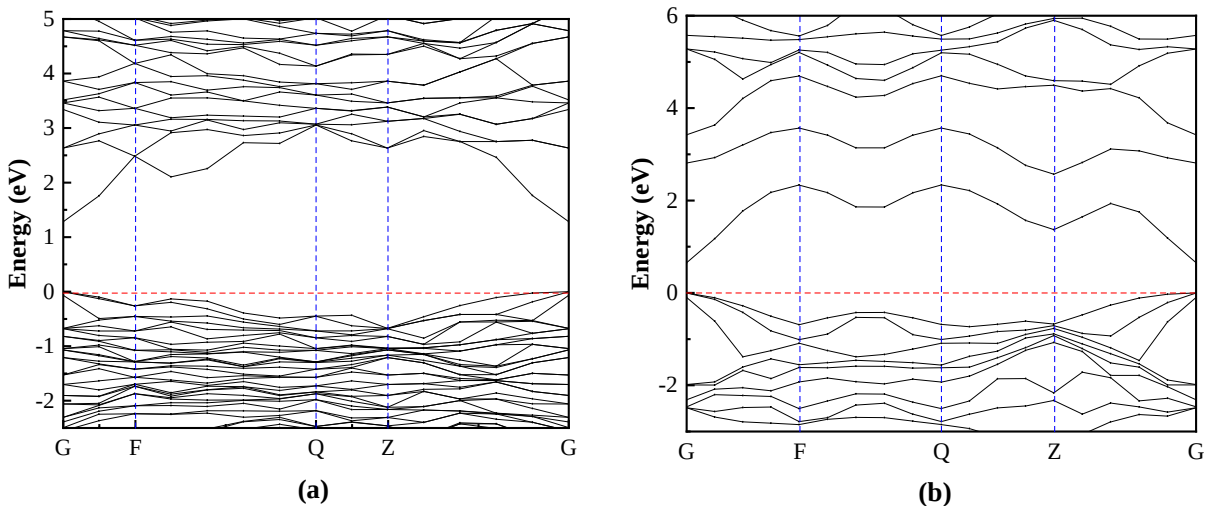

Figure 3. Energy band structure: (a) CIS, (b) CIS:Tl

Fig. 4 shows a comparison of the density of states of the primary cell CIS and CIS:Tl. The effect of doping elements on the electronic structure and bandgap properties of the CIS:Tl system can be better understood by analysing the fractional density of states of CIS:Tl [19]. From Fig. 4b, a total of seven peaks appear in the CIS:Tl total density of states plot, and the CIS:Tl total density of states plot changes at the same rate as that of the primary CIS in the range less than 10 eV, with no energy levels appearing in the CIS:Tl system beyond 10 eV. As can be seen from Fig. 4c, peak 1 (-15 eV ~ -13.75 eV) originates mainly from the 3s state of the S atom; the 4d state of the In atom and the 5d state of the Tl atom make up peak 2 (-13.75 eV ~ -12.5 eV), peak 3 (-12.5 eV ~ -11.25 eV) is mainly derived from the 3s state of the S atom, peak 4 (-6.25 eV ~ -5 eV) and peak 5 (-2.5 eV ~ 0 eV) are The doping of Tl leads to a partial narrowing of the conduction band of CIS and the introduction of some impurity levels in the valence band near the Fermi energy level.

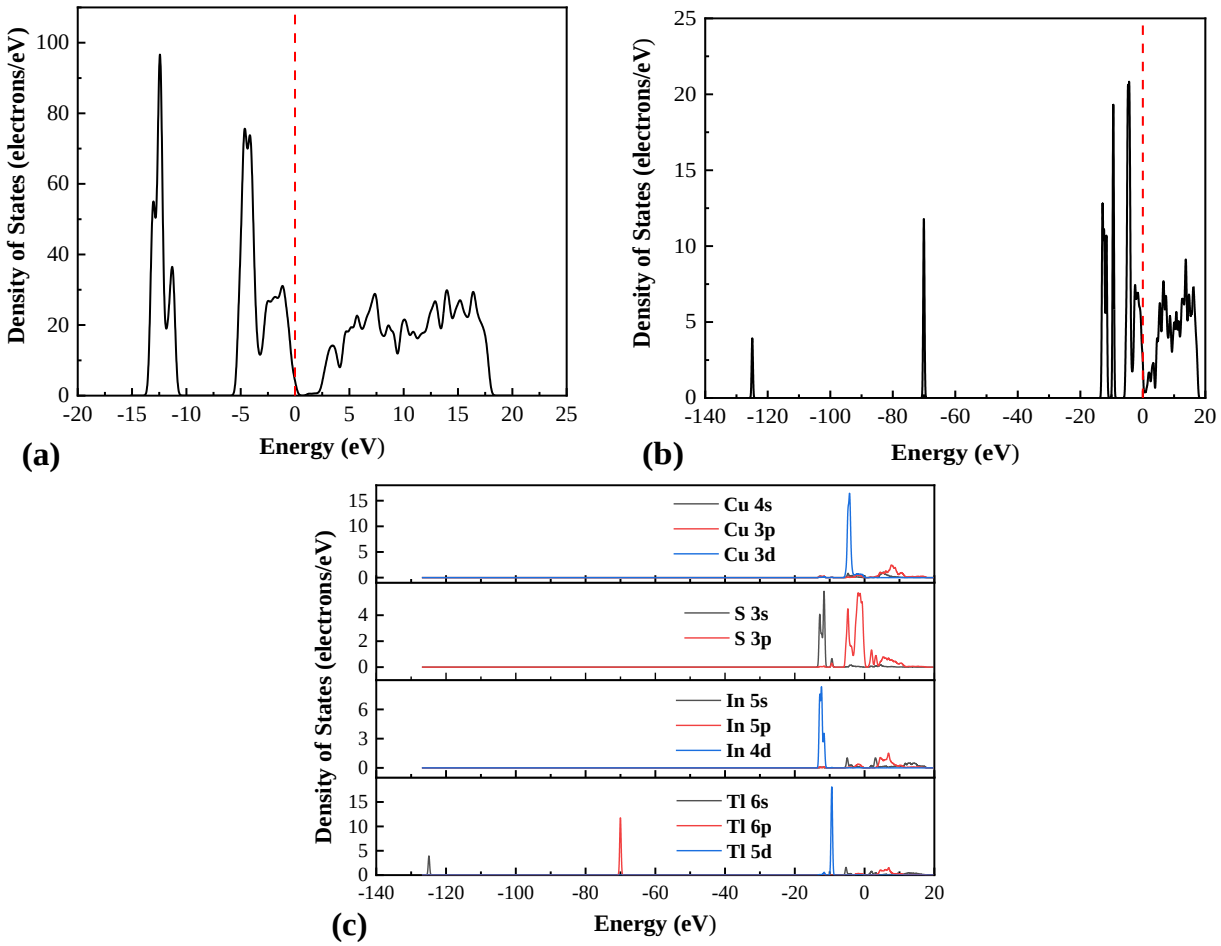

Figure 4. Density of states diagram (a) protocell CIS, (b) CIS:Tl, (c) partial wave

3.2. Analysis of the optical properties of Tl-doped $CuInS_2$

As shown in Fig. 5, the dielectric function curves of the original cell CIS and the Tl-doped CIS are plotted as a function of frequency, where the black squares represent the dielectric function of the original cell CIS and the red triangles represent the dielectric function of the Tl-doped CIS. As can be seen from Fig. 5, the main peak value in the dielectric function graph of the original cell CIS splits into two peaks of 11.9 eV and 4.8 eV after doping with the Tl element, after which the trend of the change in the dielectric function curve of both remains the same. The analysis of the energy band diagram and the density of split states of CIS:Tl shows that the peak of the permittivity function at 4.8 eV mainly originates from the introduction of electrons in the Tl-6p state, and the peak of the permittivity function at 11.9 eV is formed by electrons in the Tl-5d state.

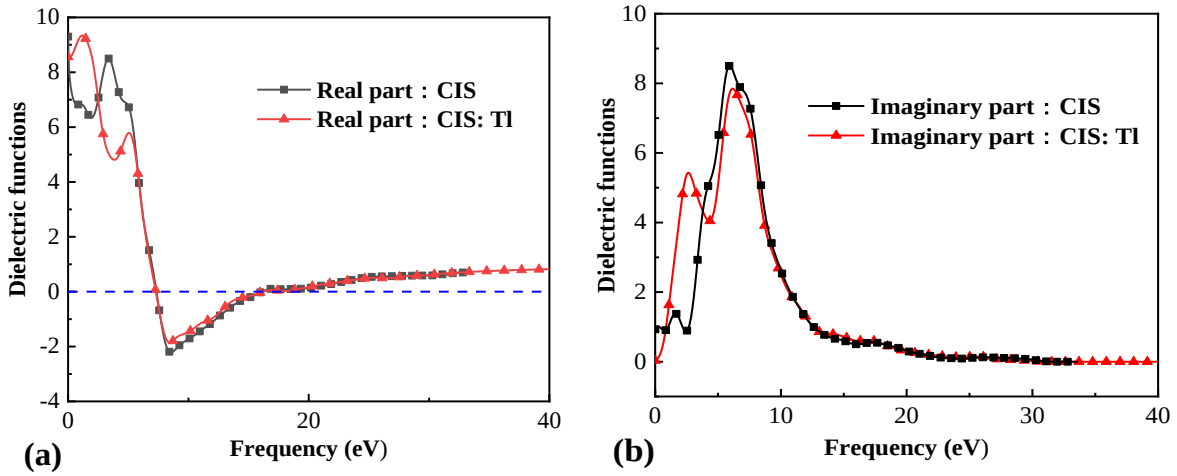

Figure 5. Comparison diagram of dielectric function (a) real part, (b) imaginary part

In order to further analyze the influence of Tl atom doping on the optical properties of CIS, the absorption [20] spectra of protocell CIS and CIS: Tl are calculated and compared, as shown in Fig. 6. It can be seen from the Fig. 6 that the main absorption peak of protocell CIS is at 24.9 eV, and the main absorption peak of CIS:Tl is at 27.2 eV. It was also observed that the absorption peak of CIS doped with Tl moves towards the high energy direction, resulting in a blue shift. At the same time, it is found that the absorption intensity of the main absorption peak of protocell CIS is less than CIS:Tl, which is caused by lattice relaxation after doping. Compared with protocell CIS, the number of absorption peaks of CIS: Tl increases, but the number of main absorption peaks is consistent with that of protocell CIS, which shows that the doping of Tl will only affect the position and intensity of absorption peaks of CIS.

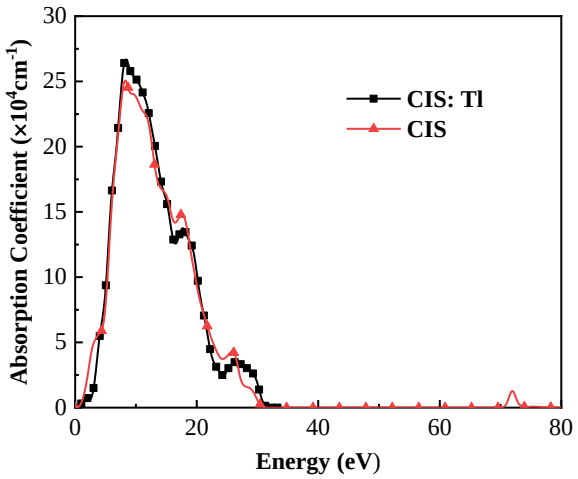

Figure 6. Comparison of the absorption coefficients of proto-cell CIS and CIS: Tl

The conductivity of the material is a technical parameter indicating the difficulty of charge flow in an object [21]. In the formula, the conductivity is written in Greek letters σ To express. The standard unit of is Siemens / meter (abbreviated as S/m). Element doping has a great impact on the conductivity of solid-state semiconductors, which affect the performance of semiconductor thin-film solar cells. As

shown in Fig. 7, the conductivity of protocell CIS and CIS:Tl were calculated and compared. It can be seen from the Fig. 7 that before and after element doping, the real part and imaginary part of their conductivity tend to be roughly the same. Among them, the real peak value of protocell CIS conductivity is 6.16 S/m. After Tl element doping, the peak value of CIS:Tl conductivity reaches 6.78 S/m, which shows that Tl doping can significantly improve the peak value of CIS conductivity, and the peak value of conductivity after doping is increased by 10.06%.

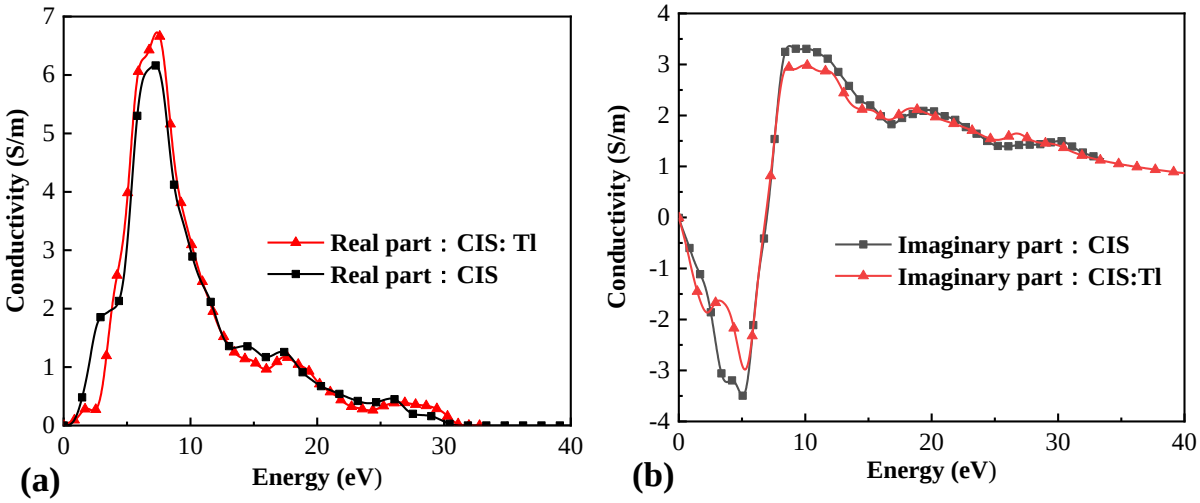

Figure 7. The comparison of conductivity ,(a) real part, (b) imaginary part

4. CONCLUSION

CIS semiconductor thin film materials have significant advantages such as low cost and excellent optical properties, and have a wide application prospect in the field of solar electric vehicles. For the unclear mechanism of the performance regulation of CIS semiconductor thin film materials, this paper adopts the Tl doping method to regulate the CIS photoelectric properties, and derives the lattice constants, electronic structure and optical properties of proto-cell CIS and CIS:Tl based on the first principle calculation method. The main conclusions can be drawn as follows.

(1) Tl-doped CIS is still a direct bandgap semiconductor and the band gap value is reduced by 33.4% compared to the band gap value of the original cell CIS, mainly due to the introduction of impurity energy levels in the Tl element and the impurity energy levels will hybridize with the original energy levels. The reduced bandgap value will make the crystal red-shift its luminescence wavelength.

(2) The absorption peak of Tl-doped CIS is shifted to the high-energy region and the absorption intensity of the main absorption peak is increased by 8.4% compared with that of the original cell CIS. The increase in absorption intensity is beneficial to enhance the ability of CuI-Si solar cells in the process of absorbing sunlight, and the efficiency of the cells in absorbing light is improved.(3) Tl-doped CIS has 10.06% higher peak electrical conductivity in real part compared to the original cell CIS, which can also improve the crystallization of the film and increase the solar cell efficiency.

References

1. S.L. Castro, S.G. Bailet, R.P. Raffaelle, K.K. Banger and A.F. Hepp, *J. Phys. Chem. B.*, 33 (2004) 12429.
2. T. Omata, K. Nose, K. Kurimoto and M. Kita, *J. Mater. Chem. C.*, 33 (2014) 6867.
3. I.T. Kraatz, M. Booth, B.J. Whitaker, M.G.D. Nix and K. Critchley, *J. Phys. Chem. C.*, 41 (2014) 24102.
4. H. Chen, C.Y. Wang, J.T. Wang, X.P. Hu and S.X. Zhou, *J. Appl. Phys.*, 8 (2012) 84513.
5. W.D. Rice, H. McDaniel, V.I. Klimov and S.A. Crooker, *J. Phys. Chem. Lett.*, 23 (2014) 4105.
6. Uehara Masato, Watanabe Kosuke, Tajiri Yasuyuki, Nakamura Hiroyuki, and Maeda Hideaki, *J. Chem. Phys.*, 13 (2008) 134709.
7. J.L. Shay and H.M. Kasper, *Phys. Rev. Lett.*, 17 (1972) 1162.
8. S. Kono and M. Okusawa, *J. Phys. Soc. Jpn.*, 5 (1974) 1301.
9. C. Rincon and R. Marquez, *J. Phys. Chem. Solids.*, 11 (1999) 1865.
10. H.S. Choi, Y. Kim, J.C. Park, D.Y. Jeon and Y.S. Nam, *RSC Adv.*, 54 (2015) 43449.
11. R.D. Shannon, *Acta Crystallogr., Sect. A: Found. Crystallogr.*, 32(1976) 751.
12. Q. Zhao, Q. Feng and Y.M. Gao, *J. Wuhan Univ. Technol. Mater. Sci. Ed.*, 35(2013) 6.
13. G.C. Park, H.D. Chung, C.D. Kim, H.R. Park, W.J. Jeong, J.U. Kim, H.B. Gu and K.S. Lee, *Sol. Energy Mater. Sol. Cells*, 49 (1997) 365.
14. K. Siemer, J. Klaer, I. Luck, J. Bruns, R. Klenk and D. Bräunig, *Sol. Energy Mater. Sol. Cells*, 67 (2001) 159.
15. J.L. Yuan, C. Shao, L. Zheng, M.M. Fan, H. Lu, C.J. Hao and D.L. Tao, *Vacuum*, 99 (2014) 196.
16. T. Abe, S. Kohiki, K. Fukuzaki, M. Oku and T. Watanabe, *Appl. Surf. Sci.*, 174 (2001) 40.
17. X.J. Liu, J.C. Yang, G.X. Jia, C.Q. Yang and C.K. Cai, *J. Mater. Eng.*, 47 (2019) 72.
18. L.C. Jia, Y.B. Wang, Q.Q. Nie, B. Liu, E.Z. Liu, X.Y. Hu and J. Fan, *Mater. Lett.*, 200 (2017) 27.
19. B. Koo, R.N. Patel, and B.A. Korgel, *Chem. Mater.*, 21 (2009) 1962.
20. W.D. Rice, H. McDaniel, V.I. Klimov and S.A. Crooker, *J. Phys. Chem. Lett.*, 5 (2014) 4105.
21. M.B. Rabenh, N. Khedmi, M.A. Fodha and M. Kanzari, *Energy Procedia*, 44 (2014) 52.